

Electronic Supporting Information (ESI) for

**Crosslinked High-Performance Anion Exchange Membranes based on
Poly(dibenzyl *N*-methyl piperidine) and Pentafluorobenzoyl-Substituted SEBS**

Soomin Jeon,^{a,b,1} SeongMin Han,^{c,1} Junghwa Lee,^{a,b} Kyungwhan Min,^{a,b} Sang Yong Nam,^{c,*}

and Tae-Hyun Kim ^{a,b,*}

^a Organic Material Synthesis Laboratory, Department of Chemistry, Incheon National University, 119
Academy-ro, Yeonsu-gu, Incheon, 22012, South Korea

^b Research Institute of Basic Sciences, Core Research Institute, Incheon National University, 119
Academy-ro, Yeonsu-gu, Incheon, 22012, South Korea

^c Department of materials Engineering and Convergence Technology, Gyeongsang National University,
Jinju 52828, Republic of Korea

Experimental Section

Materials. Dibenzyl (99%) and trifluoromethanesulfonic acid (98%) were purchased from TCI (Tokyo, Japan). Triethylsilane (98%) and pentafluorobenzoyl chloride (98%) were obtained from Alfa Aesar (Haverhill, MA, USA). *N*-methyl-4-piperidone (97%), aluminum chloride (99%), 6-bromohexanoyl chloride, and trimethylamine solution (45 wt.% in H₂O) were purchased from Sigma-Aldrich (St. Louis, MO, USA). Trifluoroacetic acid was obtained from Daejung Chemicals & Metals (Siheung-si, South Korea). Poly(styrene-*b*-ethylene-*co*-butylene-*b*-styrene) (SEBS, A1535 H) with a styrene content of 57 wt.% and an M_n of 270,000 (measured via GPC using THF) was obtained from Kraton (Houston, TX, USA). All chemicals were directly used without further purification.

Synthesis of poly(dibenzyl *N*-methyl piperidine) 2. Dibenzyl (5.00 g, 27.43 mmol) and *N*-methyl-4-piperidone (3.72 g, 32.92 mmol) were taken in a dry 50-mL two-neck round-bottom flask with a magnetic stirrer and dissolved in distilled dichloromethane (20 mL). After the mixture was dissolved, the mixture was cooled to 0 °C in an ice bath. Trifluoroacetic acid (4.69 g, 41.15 mmol) and trifluoromethanesulfonic acid (41.17 g, 274.33 mmol) were slowly added to the solution in the ice bath. After 24 h, the viscous solution was poured into a large amount of 1M KOH solution. The precipitated polymer was filtered and washed with DI water several times. The polymer was filtered and dried in a vacuum oven at 80 °C overnight, which yielded poly(dibenzyl *N*-methyl piperidine) **2** as a brown powder (7.23 g, 88.0%); δ H (400 MHz, CDCl₃) 7.25–6.71 (8H, broad signal, H_{1,2}), 3.13–2.77 (4H, d, H_{3,3'}), 2.75–2.24 (8H, broad signal, H_{5,5',6}), 2.21–1.66 (4H, d, H_{4,4'}).

Synthesis of bromohexanoyl SEBS 4. SEBS (10.00 g, 54.73 mmol) was poured into a 1000 mL two-neck round-bottom flask with a magnetic stirrer under a nitrogen atmosphere and dissolved in dichloromethane (320 mL). After the polymer was fully dissolved, aluminum chloride (5.47 g, 41.05 mmol) and 6-bromohexanoyl chloride (8.76 g, 41.05 mmol) in dichloromethane (80 mL) were slowly added using a dropping funnel. After 24 h, the reaction mixture was poured into a large amount of ethanol (1500 mL), and the precipitated polymer was filtered onto filter paper and washed with ethanol several times to remove any residual reactants. The obtained polymer was dried in a desiccator at room temperature for 24 h, and this yielded bromohexanoyl SEBS **4** as a white rubbery product with a 70% molar ratio of bromohexanoyl-functionalized side chains (16.63 g, 99.1%); δ H (400 MHz, CDCl₃) 7.97–7.39 (2H, broad signal, H₆), 7.26–6.31 (4H, broad signal, H_{7–10}), 3.50–3.38 (2H, broad signal, H₁), 3.04–2.78 (2H, broad signal, H₅), 2.74–2.35 (1H, broad signal, H₁₂), 2.05–0.53 (33H, broad signal, H_{2–4,11,13–18}).

Synthesis of bromohexyl SEBS 5. Bromohexanoyl SEBS **4** (16.00 g, 38 mmol) was poured into a 1000-mL two-neck round-bottom flask connected to a reflux condenser and fitted with a magnetic stirrer under a nitrogen atmosphere. Then, it was dissolved in chloroform (320 mL). After the polymer was fully dissolved, triethyl silane (60.70 mL, 380 mmol) and trifluoroacetic acid (58.16 mL, 760 mmol) were added. The reaction mixture was slowly heated to 105 °C and left for 24 hours at this temperature. The reaction mixture was cooled to room temperature, and 1 M KOH (400 mL) was added to neutralize the solution. The organic layer was poured into methanol (1500 mL), and the precipitated polymer was filtered onto filter paper and washed with methanol several times to remove any residual reactants. The obtained polymer was dried in a desiccator at room temperature for 24 h, and the bromohexyl SEBS **5** appeared as a white rubbery product (15.27 g, 93.1%); δ H (400 MHz, CDCl₃) 7.22–6.21 (7H, broad signal, H_{6–10}), 3.48–3.34 (2H, broad signal, H₁), 2.66–2.25 (3H, broad signal, H_{5',12}), 1.95–0.60 (33H, broad signal, H_{2–5, 11, 13–18}).

Synthesis of Br-Hex-m-F5-SEBS 3. Bromohexyl SEBS **5** (2.00 g, 6.74 mmol) was poured into a 250-mL two-neck round-bottom flask with a magnetic stirrer under a nitrogen atmosphere and dissolved in dichloromethane (80 mL). After it was fully dissolved, aluminum chloride (0.27 g, 2.02 mmol) and pentafluorobenzoyl chloride (0.54 g, 2.36 mmol) were poured into dichloromethane (40 mL) and the solution was slowly added using a dropping funnel. After 4 h, the reaction mixture was poured into a large amount of methanol, and the precipitated polymer was washed with methanol several times. The product polymer was dried in a desiccator at room temperature for 24 h, and Br-Hex-m-F5-SEBS **3** was a white rubbery product (2.27 g, 92.8%); δ H (400 MHz, CDCl₃) 7.65–7.35 (0.19H, broad signal, H₂₀), 7.23–6.18 (6H, broad signal, H_{6–10}), 3.47–3.33 (2H broad signal, H₁), 3.05–2.83 (1H broad signal, H₁₉), 2.67–2.30 (3H, broad signal, H_{5',12}), 1.96–0.57 (31H broad signal, H_{2–5,11,13–18}).

Characterization and measurements. The chemical structures of the synthesized poly(dibenzyl *N*-methyl piperidine) **2** and Br-Hex-m-F5-SEBS **3** were identified via ¹H NMR spectroscopy and Fourier transform infrared (FTIR) spectroscopy. ¹H NMR spectra were obtained using a 400 MHz NMR instrument (Agilent 400-MR) using a CDCl₃ as a reference. FTIR spectra were obtained using a PerkinElmer Spectrum Two ATR-FTIR spectrometer. Spectra were collected from 4000 to 400 cm⁻¹.

Intrinsic viscosity measurement. The polymer's intrinsic viscosity (η) was measured at 25 °C using a Schott Viscometry System (AVS 370, Germany) in a CHCl₃ solution. The Schott ViscoSystem (AVS 370, Germany) consists of an Ubbelohde viscometer (SI Analytics, Type 532 03) and automatic piston burette (TITRONIC universal). A 3.5 mg/cm³ polymer solution was prepared by dissolving a sample in CHCl₃. The efflux time of the solution was then recorded three times. The time of flow out (t_1) for each sample,

and the time of solvent flow out (t_0) were determined at 25 °C. Taking the c as the x-axis, the reduced viscosity (η_{red}) and inherent viscosity (η_{inh}) as the y-axis, draw two curves and extrapolated η_{red} and η_{inh} to $c = 0$. The intrinsic viscosity was calculated from the y-intercept. The η_{red} and η_{inh} were calculated from Equation 1 and 2:

$$\eta_{red} = \frac{\left(\frac{t_1}{t_0} - 1\right)}{c} \#(1)$$

$$\eta_{inh} = \frac{\left(\frac{t_1}{t_0} - 1\right)}{c} \#(2)$$

where t_1 is the outflow time of polymer solution, t_0 is the outflow time of solvent, and c is the polymer concentration.

IEC. The IEC values of each membrane in OH^- form were determined by acid–base back titration. The samples in OH^- form were washed with DI water several times and immersed in 10 mL of a 0.01 M HCl standard aqueous solution for at least 24 h to neutralize the OH^- . Then, the membranes were removed and dried in a 40 °C vacuum oven for 24 h. The residual HCl solution was titrated with a 0.01 M NaOH standard aqueous solution, using a phenolphthalein indicator. Equation 3 was used to determine the experimental IEC (meq g^{-1}):

$$IEC (\text{meq g}^{-1}) = \frac{(V_0 \times C_0 - V_{KOH} \times C_{KOH})}{W_{dry}} \#(3)$$

where V_0 (mL) and C_0 (M) are the volume and concentration of the HCl standard aqueous solution, respectively; V_{KOH} and C_{KOH} are the volume and concentration of the KOH standard aqueous solution in the back titration, respectively; and W_{dry} (g) is the weight of the membrane after drying in an oven at 40 °C for 24 h.

Water uptake (WU) and swelling ratio (SR). The WU (%) and swelling ratio (SR, %) were calculated for each membrane by soaking the circular membranes in water at 20 °C and 80 °C. The membranes in their OH^- form were immersed in DI water for at least 24 h, the surface of the membranes was wiped dry with a tissue, the samples were quickly weighed (W_{wet} , g), and the length (L_{wet} , cm) and thickness (T_{wet} , mm) were immediately measured. The membranes were dried under vacuum for 24 h, and the weight (W_{dry} ,

g), length (L_{dry} , cm), and thickness (T_{dry} , mm) of the dry membranes were also recorded. Equations 4 and 5 were used to determine the WU (%) and SR (%), respectively:

$$WU (\%) = \frac{W_{wet} - W_{dry}}{W_{dry}} \times 100 \#(4)$$

$$SR (\%) = \frac{L_{wet} - L_{dry}}{L_{dry}} \times 100 \text{ or } \frac{T_{wet} - T_{dry}}{T_{dry}} \times 100 \#(5)$$

The hydration number (λ) of each membrane was calculated from the WU value and experimental IEC, according to Equation 6:

$$\text{Hydration number } (\lambda) = \frac{\text{Water uptake } (\%) \times 1000}{IEC \times 18} \#(6)$$

Contact angle. The contact angle of each membrane was measured statically on a Surface Electro Optics instrument and calculated using SEO Surfaceware-9. The membrane was placed on a flat surface to determine the contact angle. Subsequently, an 11- μ L drop of water was placed on the surface of the membrane. A photograph was taken 10 seconds after the water droplet touched the surface to measure the contact angle.

Morphological analysis. The morphology of each membrane was analyzed using a field emission transmission electron microscope (FE-TEM, Talos F200X, Thermo Fisher Scientific, Waltham, MA, USA) image collected at an accelerating voltage of 200 kV. The samples were prepared as follows: 3–4 drops of 1 wt% polymer solution in $CHCl_3$ were placed on a copper grid to make a thin homogeneous film. The grid was dried at 40 °C for 12 h and then treated with TMA solution at 45 °C for 12 h. After TMA treatment, the grid was washed with DI water to remove excess TMA and dried in a 40 °C oven.

Small-angle X-ray diffraction (SAXS). SAXD spectra of the dry membranes were collected using a Rigaku HR-XRD Smart Lab diffractometer employing a scanning rate of 0.1°/min in the 2θ range of 0° to 4° using Cu $K\alpha$ X-rays ($\lambda = 1.5412 \text{ \AA}$). The dried membranes were placed under vacuum at 40 °C for 12 h before the measurement.

Mechanical properties, thermal stability, and hydrogen permeability. A benchtop tensile tester (Shimadzu EZ-TEST E2-L, Kyoto, Japan) was used to measure the mechanical properties of the membranes in their Br^- form at a crosshead speed of 10 mm min^{-1} at 25 °C under 50% RH. The cross-sectional area of the samples in their initial state was used to determine the engineering stress. The initial slope of the stress–strain curve was used to calculate Young’s modulus (E). For this test, samples of each membrane were

prepared in dumbbell shapes of 40×10 mm total area and 20×10 mm test area.

The thermal stability of the membranes was investigated by thermogravimetric analysis (TGA) using a Scinco TGA N-1000 instrument (Seoul, Korea) at a heating rate of $10\text{ }^{\circ}\text{C min}^{-1}$ from $30\text{--}800\text{ }^{\circ}\text{C}$ under a nitrogen atmosphere.

The glass transition temperature (T_g) of each membrane was measured by differential scanning calorimetry (DSC) using a PerkinElmer DSC 4000 (Waltham, MA, USA). Samples were prepared in aluminum pans and analyzed from -40 to $200\text{ }^{\circ}\text{C}$ for two cycles with heating and cooling rates of $10\text{ }^{\circ}\text{C min}^{-1}$. T_g was determined from the second heating cycle.

H_2 permeability measurements were carried out using the traditional constant volume/variable pressure method at room temperature (RT) under dry and humidified conditions by slightly modifying the method described in the literature. The measurement was repeated more than three times for each membrane using different specimens, and the average value was used for subsequent calculations. The H_2 permeability was calculated using Equation 7:

$$\text{Permeability (barrer)} = DS = \frac{V_p^l (P_{p2} - P_{p1})}{\left[ART \Delta t \left(P_f - \frac{P_{p2} - P_{p1}}{2} \right) \right]}, \#(7)$$

where D is the H_2 gas diffusivity coefficient ($\text{cm}^2 \text{S}^{-1}$), S is the solubility coefficient [$\text{cm}^3 (\text{cm}^2 \text{scmHg})^{-1}$], V_p is the constant permeation volume (cm^3), l is the thickness (cm), A is the active membrane surface (cm^2), R is the universal gas constant ($\text{J mol}^{-1} \text{K}^{-1}$), T is the temperature (K), P_f is the feed pressure (cmHg), and Δt is the time for the pressure to change from P_{p1} to P_{p2} (s).

Hydroxide ion conductivity. The hydroxide ion conductivity (σ) of each membrane was measured via two-probe impedance spectroscopy using an AC impedance analyzer (SP-200, Bio-Logic SAS, Claix, France). The electrode systems were connected at frequencies from 100 mHz to 2 MHz. Rectangular samples were prepared with dimensions of 1×4 cm. The OH^- conductivity was measured using the resistance (R , Ω) in DI water from 20 to $80\text{ }^{\circ}\text{C}$. The OH^- conductivity was calculated using Equation 8:

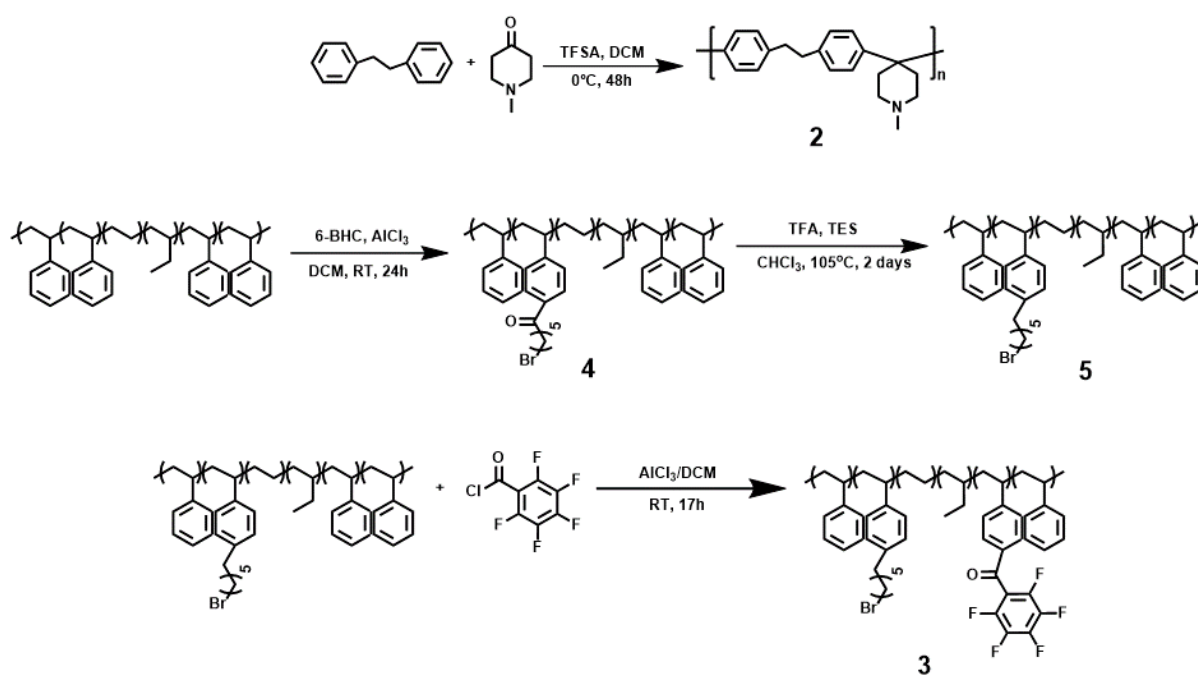
$$\sigma = \frac{L}{R \times A} \#(8)$$

where L (cm) is the distance between the reference electrodes, and A (cm²) is the cross-sectional area of the membrane.

A humidity temperature oven with a conductivity cell connected to an impedance/gain-phase analyzer was used to measure the hydroxide conductivity at 95% RH and 60 °C. The membrane between the electrodes was exposed to an RH of 95% for 2 h before each measurement.

Alkaline stability. The membranes in their OH⁻ form were soaked in a 1 M KOH solution at 80 °C for 1080 h to evaluate their chemical stability by measuring the changes in IEC, conductivity, and FTIR spectra. Before the measurements, each membrane was soaked in freshly prepared 1 M KOH solution at 60 °C for at least 24 h. After this period, the OH⁻ conductivity of each membrane was measured in DI water at 20 °C, and the IEC was measured using the back-titration method, as described in Section 2.8.

Peel test. A peel test was used to determine the adhesion properties of the MEA. The electrodes were prepared with 12-mm wide 3M tape. The adherence of the catalyst to the membrane was measured using a universal testing machine (UTM, Shimadzu) at a constant displacement rate of 20 mm min⁻¹.



Scheme S1. Synthetic routes to PDB **2**, bromohexanoyl SEBS **4**, bromohexyl SEBS **5**, and Br-Hex-m-F5-SEBS **3**

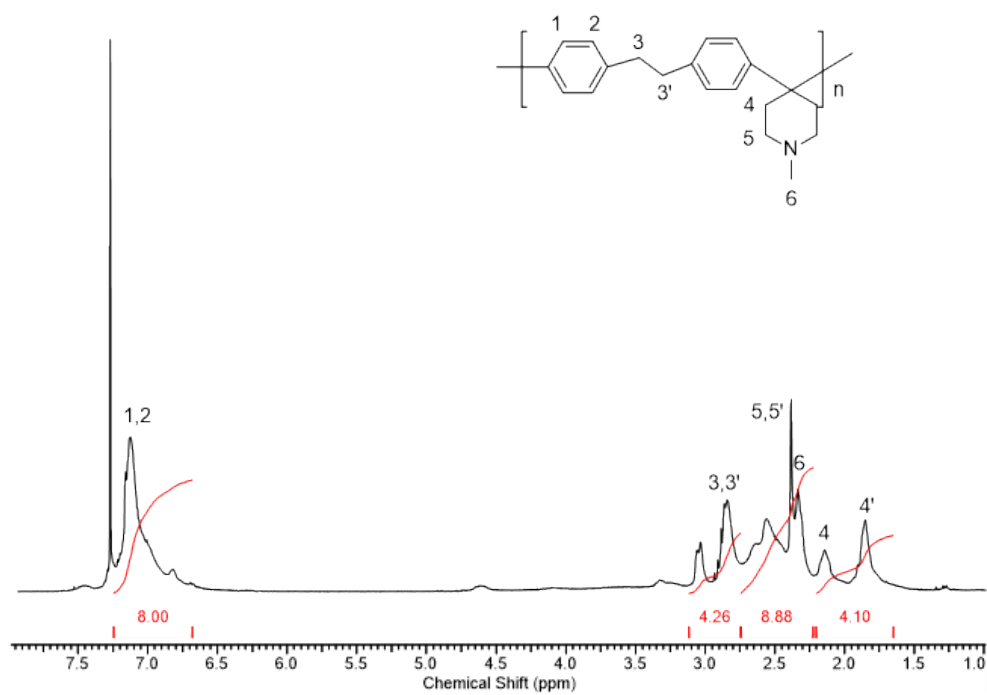


Figure S1. ^1H NMR spectrum of PDB 2

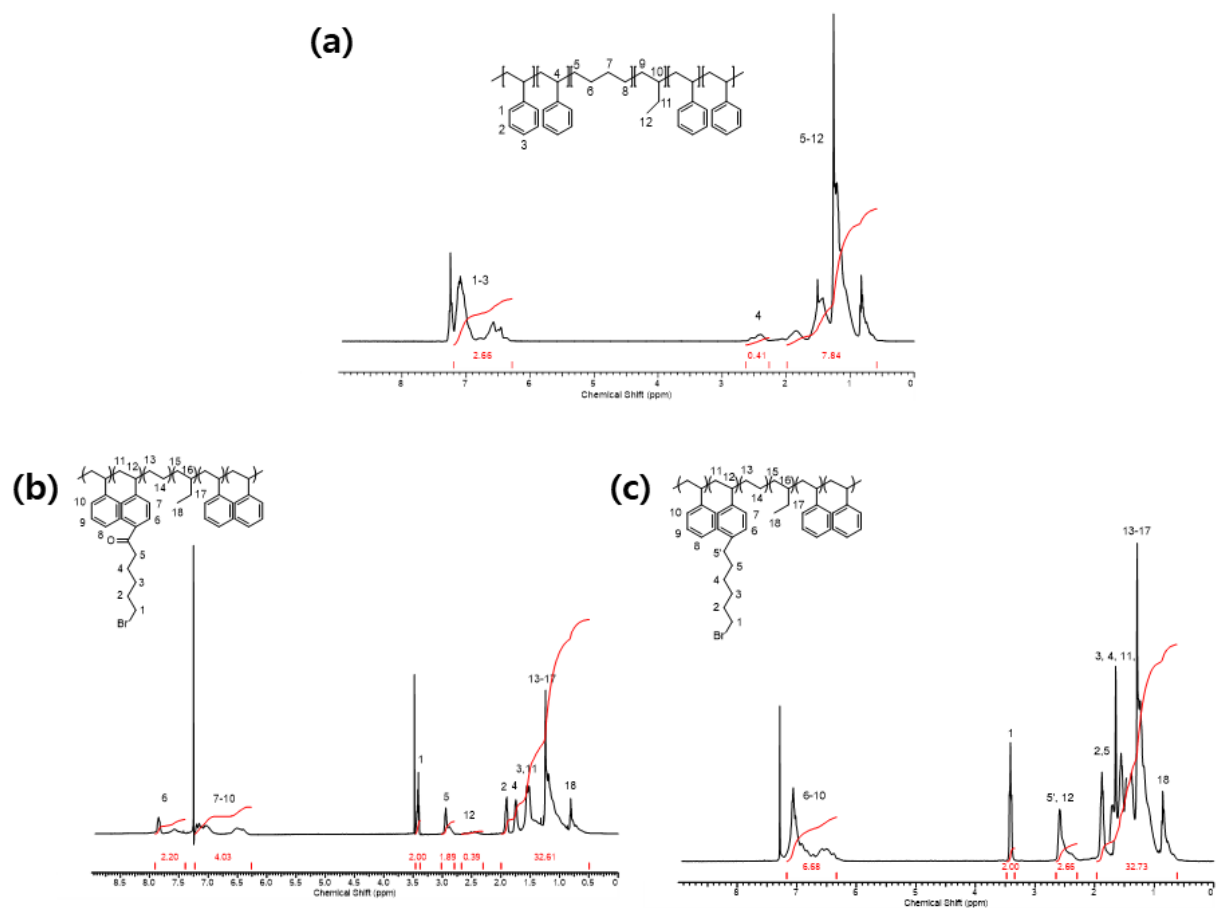


Figure S2. ^1H NMR spectra of (a) pristine SEBS, (b) bromohexanoyl SEBS **4**, and (c) bromohexyl SEBS

5

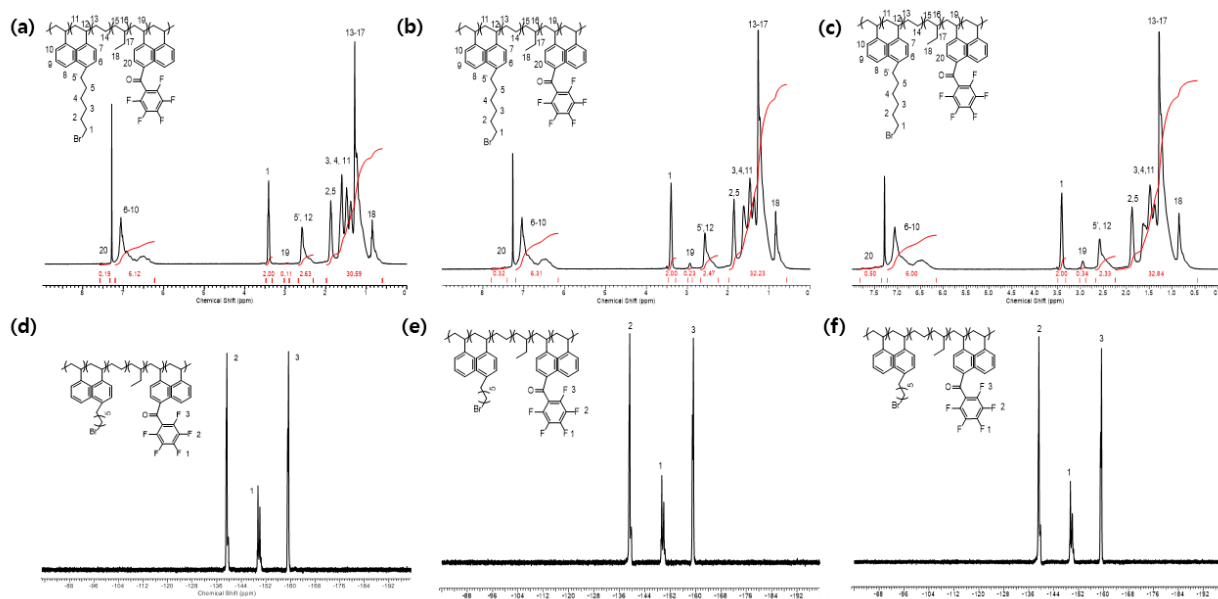


Figure S3. ^1H spectra of Br-Hex-m-F5-SEBS **3** at (a) $m=4$, (b) $m=8$, and (c) $m=12$; and ^{19}F NMR spectra of Br-Hex-m-F5-SEBS **3** at (d) $m=4$, (e) $m=8$, and (f) $m=12$

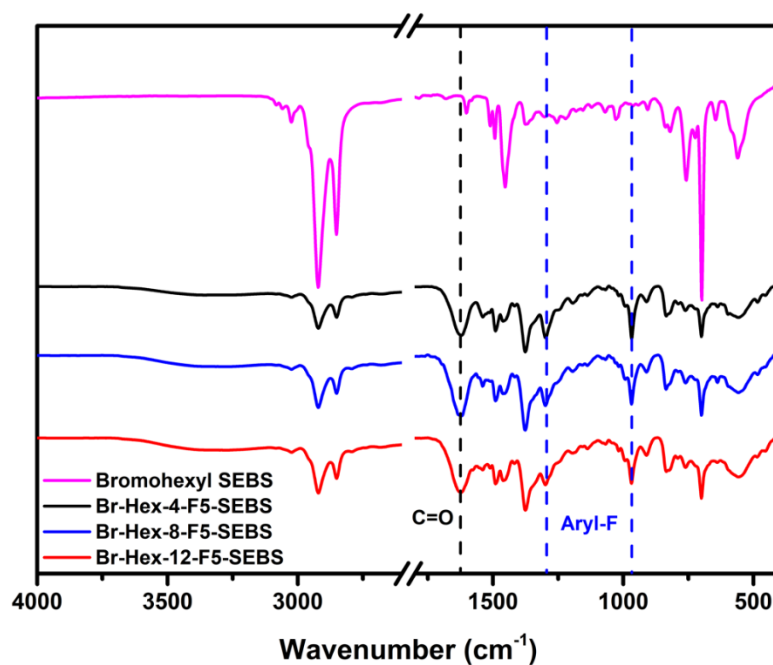


Figure S4. FT-IR spectra of bromohexyl SEBS **5** and Br-Hex-m-F5-SEBS **3**

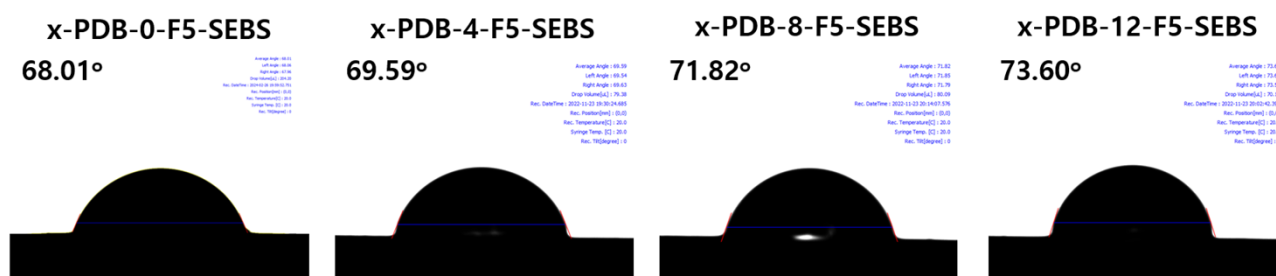


Figure S5. Contact-angle measurements of the x-PDB-m-F5-SEBS membranes with varying contents of the pentafluorobenzoyl group

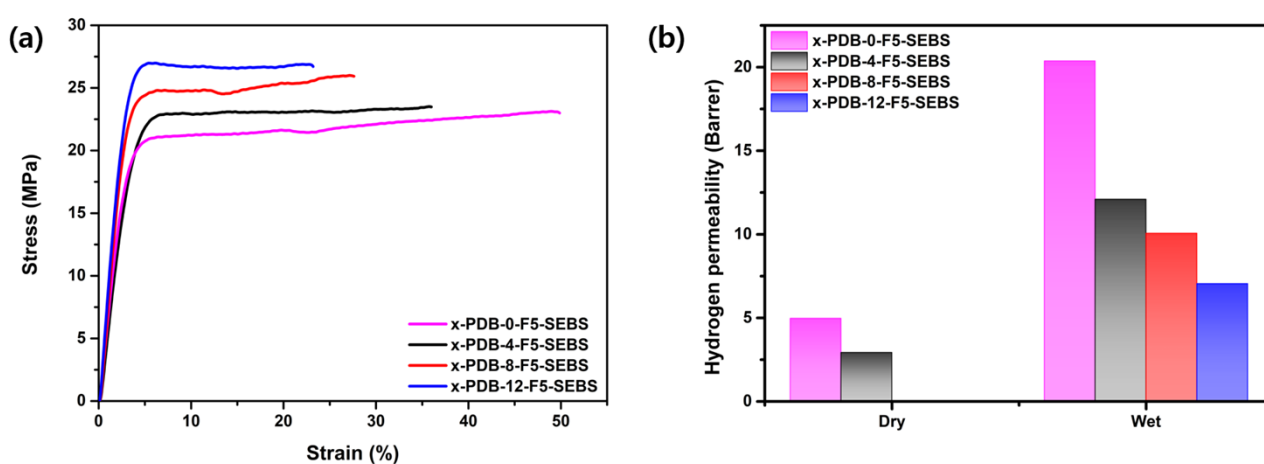


Figure S6. (a) Mechanical properties and (b) hydrogen permeability of the x-PDB-m-F5-SEBS membranes with different contents of the pentafluorobenzoyl group.

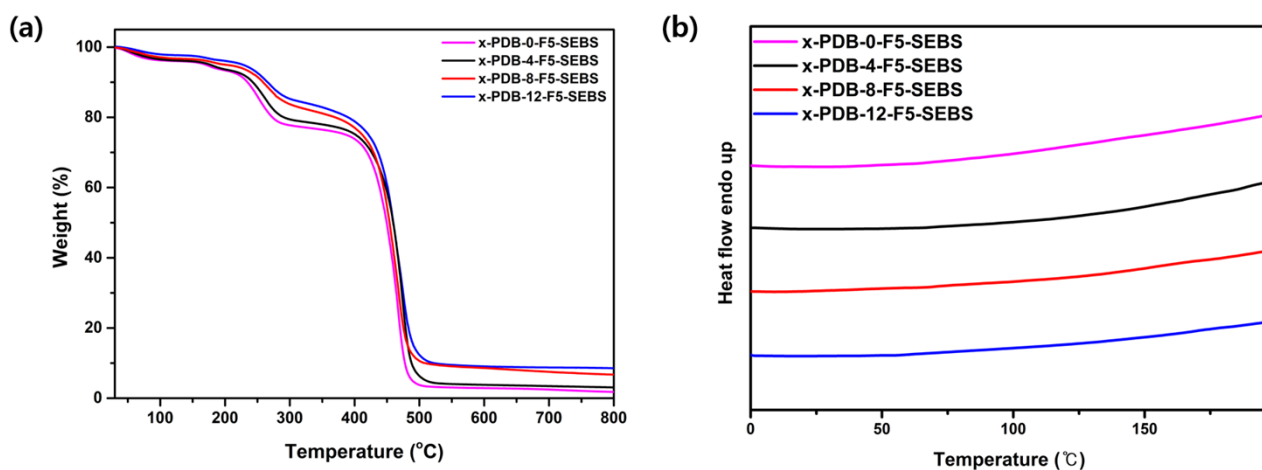


Figure S7. (a) Thermogravimetric analysis (TGA) and (b) differential scanning calorimetry (DSC) plots of the x-PDB-m-F5-SEBS membranes with different contents of the pentafluorobenzoyl group

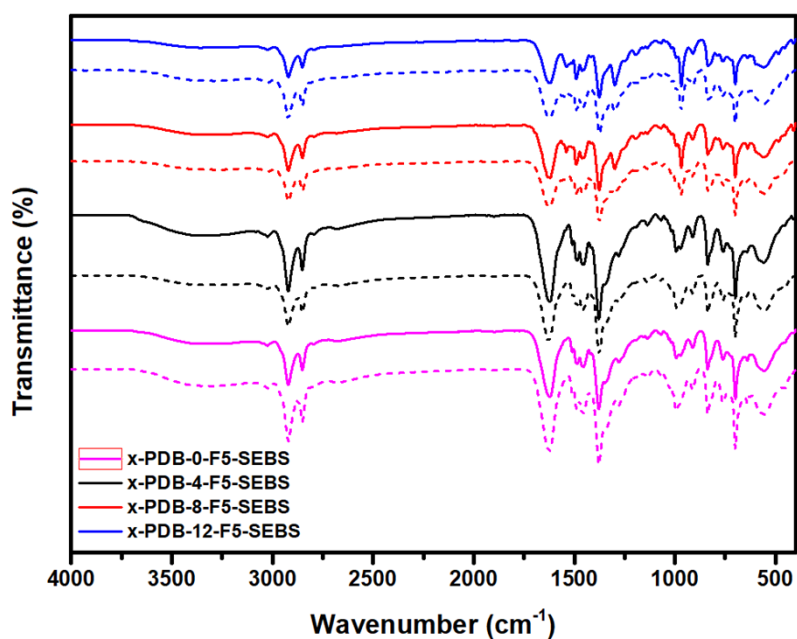


Figure S8. FT-IR spectra of the x-PDB-m-F5-SEBS membranes with different contents of the pentafluorobenzoyl group before (solid lines) and after (dashed lines) alkaline stability tests

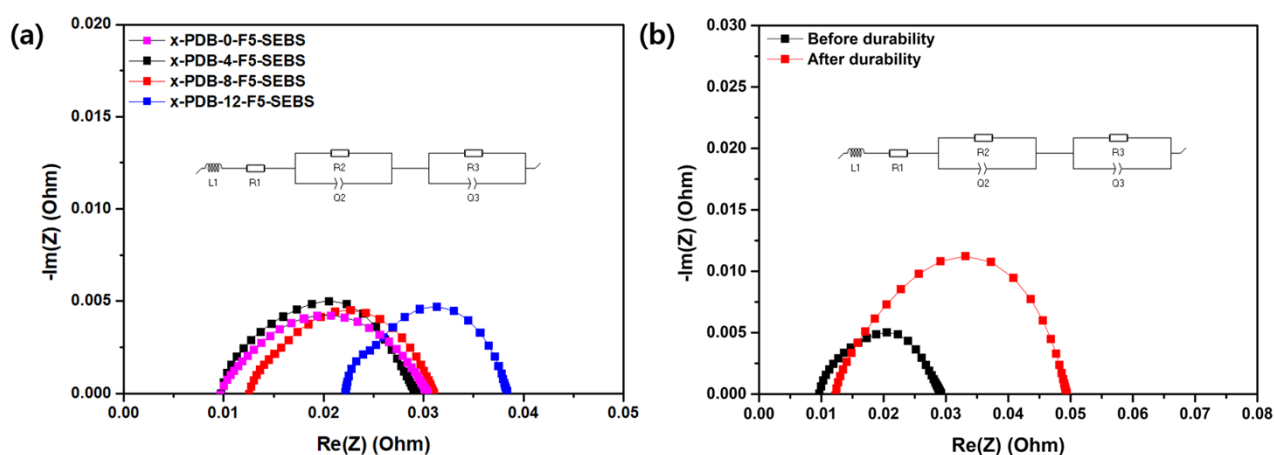


Figure S9. Nyquist plots of (a) x-PDB-m-F5-SEBS membranes and (b) x-PDB-4-F5-SEBS membranes before and after the durability tests

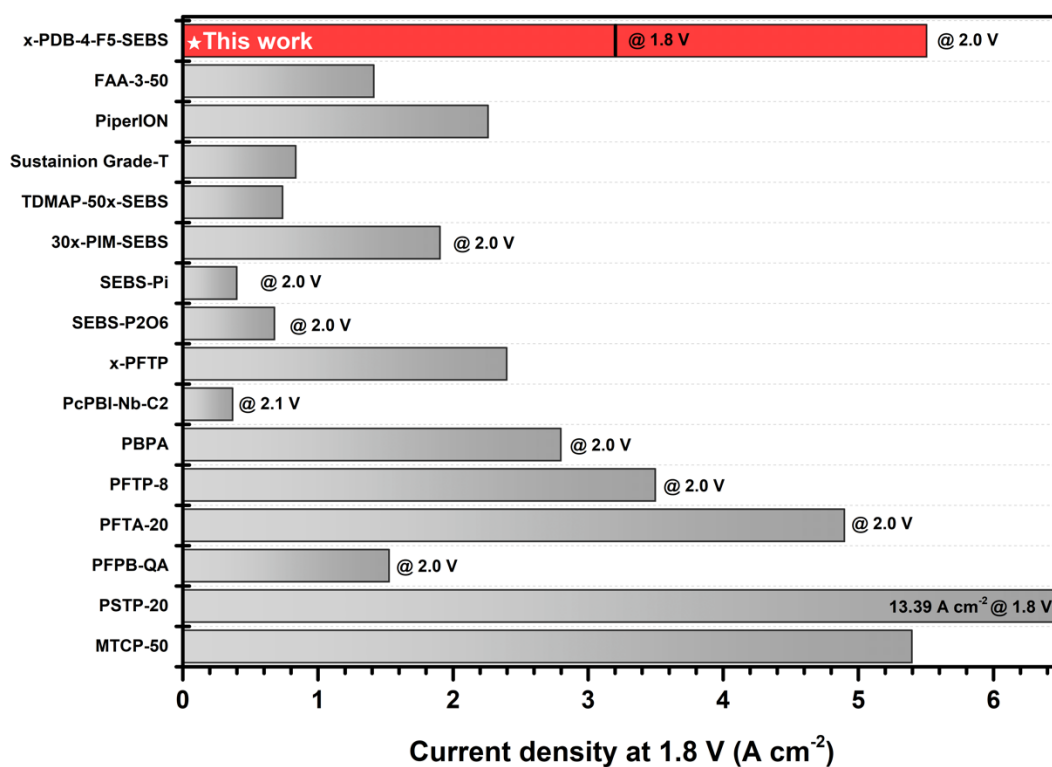


Figure S10. Comparison of AEMWE single-cell performance between x-PDB-4-F5-SEBS and commercial AEMs reported in the literature

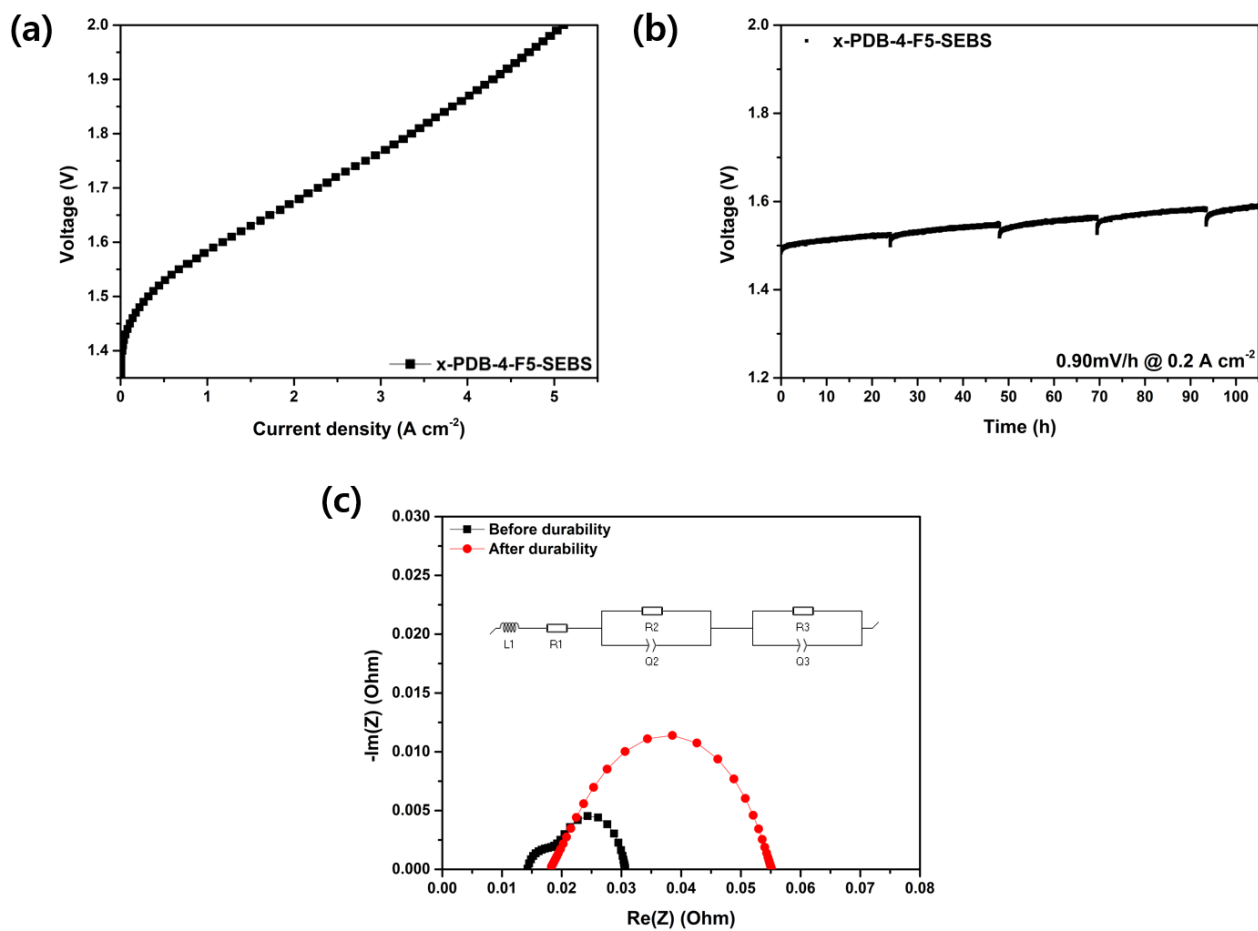


Figure S11. (a) AEMWE single-cell performance and (b) durability tests of x-PDB-4-F5-SEBS using non-precious metal catalysts for the anode, and (c) Nyquist plots of the MEAs before and after the durability tests

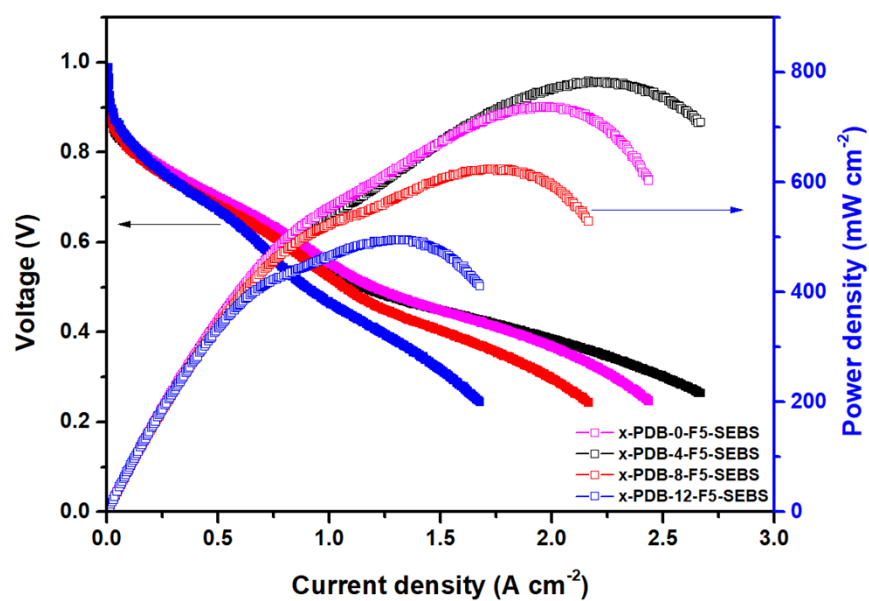


Figure S12. AEMFC single-cell performance of the x-PDB-m-F5-SEBS membranes at 60 °C and 95% RH with a 0.3/0.3 bar A/C back pressure

Table S1. SAXS profiles of the x-PDB-m-F5-SEBS membranes with different contents of the pentafluorobenzoyl group

Membrane name	Scattering vector (\AA^{-1})	d-spacing (nm)
x-PDB-0-F5-SEBS	-	-
x-PDB-4-F5-SEBS	0.02848 (1q)	22.06
	0.04842 (1.70q)	12.97
	0.05697 (2q)	11.03
	0.07904 (2.77q)	7.95
x-PDB-8-F5-SEBS	0.02848 (1q)	22.06
x-PDB-12-F5-SEBS	0.02848 (1q)	22.06

- : unmeasurable

Table S2. Mechanical properties and hydrogen permeability of the x-PDB-m-F5-SEBS membranes with different contents of the pentafluorobenzoyl group

Membrane name	Stress (MPa)	Strain (%)	Hydrogen permeability (Barrer)	
			Dry	Wet
x-PDB-0-F5-SEBS	23.00	49.86	4.97±0.46	20.37±0.73
x-PDB-4-F5-SEBS	23.48	35.99	2.93±0.13	12.10±0.38
x-PDB-8-F5-SEBS	25.93	27.61	-	10.06±0.25
x-PDB-12-F5-SEBS	26.87	22.81	-	7.05±0.01

- : unmeasurable

Table S3. Hydroxide ion conductivity of the x-PDB-m-F5-SEBS membranes with different contents of the pentafluorobenzoyl group at different temperatures

	OH ⁻ conductivity (mS cm ⁻¹)				RH conductivity ^a (mS cm ⁻¹)
	20 °C	40 °C	60 °C	80 °C	
x-PDB-0-F5-SEBS	64.92 ±0.06	89.29 ±0.09	113.94 ±0.33	135.11 ±0.33	85.19 ±0.94
x-PDB-4-F5-SEBS	60.74 ±0.28	85.27 ±0.10	110.31 ±0.30	132.62 ±0.77	99.65 ±0.90
x-PDB-8-F5-SEBS	45.25 ±0.26	61.33 ±0.07	78.60 ±0.41	92.74 ±0.58	53.69 ±0.34
x-PDB-12-F5-SEBS	40.57 ±0.05	56.38 ±0.13	69.82 ±0.41	83.86 ±0.57	45.44 ±0.71

^a The RH conductivity was measured at 60 °C and 95% RH

Table S4. Comparison of alkaline stability between the x-PDB-m-F5-SEBS membranes and AEMs reported in the literature

	AEM Type	IEC (meq g ⁻¹)	OH ⁻ conductivity ^a (mS cm ⁻¹)	Conductivity retention (%)	Conditions			Ref
					Conc. (M)	Temp. (°C)	Time (h)	
x-PDB-0-F5-SEBS	Polyarylene- SEBS crosslinked	1.86	135.11	>99	1	80	1080	This work
x-PDB-4-F5-SEBS	Polyarylene- SEBS crosslinked	1.83	132.62	>99	1	80	1080	This work
x-PDB-8-F5-SEBS	Polyarylene- SEBS crosslinked	1.78	92.74	>99	1	80	1080	This work
x-PDB-12-F5-SEBS	Polyarylene- SEBS crosslinked	1.73	83.86	>99	1	80	1080	This work

PD ₂ TP-25	Polyarylene-based	2.46	166	97	1	80	1000	[51]
QABNP	Polyarylene-based	2.60	135.25	90	2	80	1080	[52]
QAQPP	Polyarylene-based	2.29	109.12	65	2	80	1080	[52]
PTP-90	Polyarylene-based	2.50	128.9	38	1	80	960	[45]
QAPIB	Polyarylene-based	1.23	93.88	45	1	80	1050	[43]
SEBS-C16	SEBS-based	1.29	45.26	64	2	80	1700	[53]
HQA-SEBS	SEBS-based	1.51	63.6	88	1	80	500	[36]
HQA-F ₁ -SEBS	SEBS-based	1.49	71.2	94	1	80	500	[36]
HQA-F ₅ -SEBS	SEBS-based	1.45	87.0	97	1	80	500	[36]
SEBS-p-ASU-TMA-40	SEBS-based	2.16	96.6	84	2	80	2000	[37]
SEBS-a-ASU-TMA-40	SEBS-based	2.35	77.7	78	2	80	2000	[37]
10%-PBP-ASU-PPO	Crosslinked	2.31	129	86	1	80	2000	[54]
PTPBHIN-O19	Crosslinked	1.64	151.69	85	3	80	1600	[55]
CPBTT-0.6	Crosslinked	1.77	122.9	87	1	80	1080	[25]
0.9q-PTI-6C	Crosslinked	1.89	118.5	86	2	80	1200	[14]

0.9q-PTI-4C	Crosslinked	1.90	88.9	83	2	80	1200	[14]
SEBS-C16-20C4	Crosslinked	2.35	77.78	94	2	80	1700	[53]
TMHA-50x-SEBS	Crosslinked	2.11	109.9	96	2	80	864	[35]
xBEO-PPO	Crosslinked	1.93	131.96	68	1	80	620	[56]
xTEO-PPO	Crosslinked	1.91	119.88	58	1	80	620	[56]

^a OH⁻ conductivity measured at 80 °C

Table S5. Comparison of AEMWE single-cell performance between x-PDB-4-F5-SEBS and commercial AEMs reported in the literature

AEMs	Test conditions	Catalysts		Performance	Ref
		Anode	Cathode		
x-PDB-4-F5-SEBS	70°C, 1 M KOH	IrO ₂	PtRu/C	3.204 A cm ⁻² @ 1.8 V	This work
x-PDB-4-F5-SEBS	70°C, 1 M KOH	IrO ₂	PtRu/C	5.509 A cm ⁻² @ 2.0 V	This work
FAA-3-50	70°C, 1 M KOH	IrO ₂	PtRu/C	1.415 A cm ⁻² @ 1.8 V	This work
PiperION	70°C, 1 M KOH	IrO ₂	PtRu/C	2.261 A cm ⁻² @ 1.8 V	This work
Sustainion Grade-T	60°C, 1 M KOH	NiFe ₂ O ₄	Raney nickel	0.837 A cm ⁻² @ 1.8 V	[60]
TDMAP-50x-SEBS	70°C, 1 M KOH	IrO ₂	Pt/C	0.74 A cm ⁻² @ 1.8 V	[35]
30x-PIM-SEBS	70°C, 1 M KOH	IrO ₂	Pt/C	1.905 A cm ⁻² @ 2.0 V	[39]
SEBS-Pi	50°C, 5.6 wt% KOH	IrO ₂	Pt/C	0.4 A cm ⁻² @ 2.0 V	[61]

SEBS-P2O6	60°C, 1 M KOH	Ir black	Pt/C	0.68 A cm ⁻² @ 2.0 V	[62]
x-PFTP	60°C, 1 M KOH	IrO ₂	Pt/C	2.40 A cm ⁻² @ 1.8 V	[63]
PcPBI-Nb-C2	60°C, 1 M KOH	IrO ₂	Pt/C	0.37 A cm ⁻² @ 2.1 V	[64]
PBPA	60°C, 1 M KOH	IrO ₂	Pt/C	2.8 A cm ⁻² @ 2.0 V	[16]
PFTP-8	60°C, 1 M KOH	IrO ₂	Pt/C	3.5 A cm ⁻² @ 2.0 V	[63]
PFTA-20	80°C, 1 M KOH	IrO ₂	Pt/C	4.9 A cm ⁻² @ 2.0 V	[65]
PFPB-QA	70°C, 1 M KOH	IrO ₂	Pt/C	1.528 A cm ⁻² @ 2.0 V	[66]
PSTP-20	80°C, 1 M KOH	IrO ₂	PtRu/C	13.39 A cm ⁻² @ 2.0 V	[21]
MTCP-50	90°C, 1 M KOH	NiFe	PtRu/C	5.4 A cm ⁻² @ 1.8 V	[17]